

Gaia astrometric and photometric study of 3 open clusters (Collinder 467, Dolidze 18, and Ruprecht 70)

A. L. Tadross (altadross@gmail.com) & Y. H. Hendy (y.h.m.hendy@gmail.com)

National Research Institute of Astronomy and Geophysics, 11421-Helwan, Cairo, Egypt

Abstract. Here, we conducted a photometric and astrometric study of three open stellar clusters Collinder 467, Dolidze 18, and Ruprecht 70, which have not been photometrically studied before. The most important thing for using Gaia (DR2) database lies in the positions, parallax, and proper motions, which make us split cluster members from the field ones and get precise astrophysical parameters. On studying the radial density profiles of the clusters under study, the actual sizes are estimated and found larger using Gaia. From the color-magnitude diagrams and theoretical isochrones, we simultaneously determined the ages, distance moduli, and reddening of the clusters. However, considering the parallaxes of Gaia (DR2) for the cluster members, we calculated the cluster distance and confirmed what we obtained from the color-magnitude diagram. Then, the Cartesian galactocentric coordinates (X_{\odot} , Y_{\odot} , Z_{\odot}), and the distances from the galactic center (R_g) were also estimated. According to luminosity and mass functions, the total luminosity and total mass of the clusters are estimated. Our study shows that Collinder 467 is dynamically relaxed, and Ruprecht 70 has recently relaxed, while Dolidze 18 is not relaxed yet.

Keywords: (Galaxy:) open clusters and associations: individual (Collinder 467, Dolidze 18, Ruprecht 70) – database: GAIA – Photometry: Color-Magnitude Diagram – astrometry – Stars: luminosity function, mass function – Astronomical databases: miscellaneous.

1. Introduction

Open star clusters (OCs) are stellar systems that originated under the same astrophysical environments, at the same distance, with identical ages, original chemical compositions, and various masses. These objects are crucial to explaining the Milky Way Galaxy's structure and evolution (cf. Gilmore et al. 2012; Moraux 2016). Our data on OCs came from well-known global catalogs and databases, such as Dias et al. (2002, 2014) and Webda (<https://webda.physics.muni.cz/navigation.html>), which provide all the knowledge required to conduct accurate studies of such objects.

In global catalogs, there are around 3000 known open star clusters. Perhaps there are more than 100,000 OCs in our Galaxy (cf. Piskunov et al. 2006; Portegies Zwart et al. 2010; Martinez-Medina et al. 2016; Cantat-Gaudin 2020). As a result, we assume that the majority of them would be specifically found in the Gaia era. Gaia (DR2) is a high-precision database containing 1.7 billion references in the astrometric parameters of coordinates, proper motions, and parallaxes (α , δ , $\mu_{\alpha} \cos \delta$, μ_{δ} , π). Furthermore, magnitudes for over 1.3 billion references in three photometric filters (G , G_{BP} , G_{RP}), Gaia Collaboration (2018).

The Gaia Archive can be accessed via the website (<http://www.cosmos.esa.int/gaia>). As a result, we can distinguish cluster members from polluted field stars with greater precision. Using the Gaia (DR2) database, [Bossini et al. \(2019\)](#) studied the age, distance moduli, and extinction of 260 open clusters. [Cantat-Gaudin et al. \(2020\)](#) used the Gaia (DR2) database to calculate the membership probabilities of 2000 OCs, but the clusters under study were not included. Therefore, these open clusters have never been studied before using photometric data.

The candidate objects Collinder 467, Dolidze 18, and Ruprecht 70 have few astrometric studies, e.g., [Ruprecht \(1966\)](#), [Koposov et al. \(2008\)](#), [Piatti et al. \(2010\)](#), [Dias et al. \(2014\)](#), and [Sampedro et al. \(2017\)](#). Our goal is to estimate the main parameters of the three poorly studied clusters using the most recent database of the Gaia mission.

This paper is organized as follows: the data analysis is presented in Section 2. The radial density profiles (RDP), the clusters' centers, and diameters are depicted in Section 3. The color-magnitude diagrams (CMD) and photometry are performed in Section 4. Luminosity functions (LF), mass functions (MF), and the dynamical status of the clusters (the relaxation time T_R) are described in Section 5. Finally, the conclusions of our study are summarized in Section 6.

2. Data Analysis

Using the world website SIMBAD (<http://simbad.u-strasbg.fr/simbad/>) we can get the central coordinates of the clusters under study Collinder 467, Dolidze 18, and Ruprecht 70. These clusters lie in constellations Monoceros, Auriga, and Carina, respectively. They are showing no central concentration. The source data downloaded from Gaia (DR2) database service at the given centers with radii of 30, 25, and 15 arcmin, respectively. **Fig. 1** represents the optical images of the clusters under study as taken from the world-known tool ALADIN (<https://aladin.u-strasbg.fr/AladinLite>).

To minimize the impact of errors in the input data, we used sources brighter than 18-mag in G band, corresponding to typical astrometric uncertainties of 0.3 mas/yr in proper motions, and 0.15 mas in parallax as performed by [Cantat-Gauldin & Anders \(2020\)](#).

The cluster members have shared similar astrometrical properties. Thus, the vector point diagrams (VPD) of proper motion components (pmRA and pmDE) are plotted for each cluster, as shown in **Fig. 2**. The highest density area is chosen as a subset of the most probable members of the cluster. A circle has drawn around the most darkened region we selected, from which we can define the co-moving stars, [Tadross \(2018 and 2021\)](#). Co-moving stars are stars that move together with the same speed and the same direction in the sky compared to the background field ones, see **Fig. 3**. This is one of the conditions of membership that we have applied, besides the parallax, proper motions, the cluster boundary, and the CMD fitting, all of which are taken into account.

The cluster parallax range can be seen as shown in the left-hand panels of **Fig. 4**. The relation between the magnitudes and parallax shows the concentration of the cluster

members, while the stars of the field seem to be dispersed, as shown in the right-hand panels of **Fig. 4**. In this respect, a star is counted as a cluster member when located within the cluster's size (see section 3), lies within the parallax range of the cluster, and having the same velocity in the sky compared to the background field stars.

3. Cluster's structure (centers and diameters)

The cluster center is taken at the most over-density area of the cluster region. Hence, using the database of Gaia, we divided the areas of the clusters under study into equal-sized bins in RA and DE and counting the stars in each bin. Gaussian fitting profiles have been applied to both directions, as shown in **Fig. 5**. The obtained central coordinates of Collinder 467, Dolidze 18, and Ruprecht 70 are found to be in good agreement with **Dias (2002)** Catalog, listed in **Table 1**.

To obtain the diameters of the clusters under study, we divided the cluster's area into concentric circles (shells), each having a radius of 1 arcmin bigger than the previous one. The density of stars in each shell is calculated. The density distributions of the candidate clusters show good fits with the empirical **King model (1966)** that can be presented as:

$$f(R) = f_{bg} + \frac{f_0}{1+(R/R_c)^2}$$

where (f_{bg}) is the background stellar density, (f_0) is central density, and (R_c) is the core radius of the cluster, which is the distance at which the stellar density equals half the central density. The limited radius (R_{lim}) can be estimated at that value, which covers the whole cluster area and reaching sufficient constancy, where the cluster density dissolved into the background field stars, see **Fig. 6**. f_{bg} , f_0 , R_c , and R_{lim} are given in **Table 1**. On the other hand, the tidal radius of a cluster, which is the distance from the cluster core, at which the gravitational impact of the Galaxy equivalents to that of the cluster core. Calculating the total masses of Collinder 467, Dolidze 18, and Ruprecht 70 (as mentioned in Sec. 5), the tidal radius can be calculated using **Jeffries (2001)** equation:

$$R_t = 1.46 \times (M_c)^{1/3}$$

where R_t is the tidal radius (in parsec), and M_c is the total mass of the cluster (in solar mass). According to **Peterson and King (1975)**, the concentration parameter $C = \log(R_{lim}/R_c)$ shows us how the cluster is conspicuous in comparison with the background stars. It is found to be $C=1.20$, 0.93 , and 1.50 . Nonetheless, the clusters under study did not appear noticeable enough in the sky.

4. Color-Magnitude Diagram

CMD is an essential tool for estimating the fundamental parameters of the candidate clusters. Age, distance modulus, color excess, and metallicity can be estimated all at once by applying one of the Padova stellar isochrones and obtaining the best fit to the observed CMD. It is substantial to recognize the sequence of the cluster stars from the field ones because the stars in the cluster region are contaminated with background field. We used the Padova PARSEC (<http://stev.oapd.inaf.it/cgi-bin/cmd>) version 1.2S database of stellar evolutionary tracks and isochrones of **Bressan et al. (2012)**, which uses the Gaia filter

passbands of [Evans et al. \(2018\)](#). It scaled to the solar metallicity $Z=0.0152$. The best fit was obtained from the visual isochrone fit, where three suitable isochrons of different ages have been applied to each cluster as shown in [Fig. 7](#). The main parameters of Collinder 467, Dolidze 18, and Ruprecht 70 are verified with ages of 1.0 ± 0.3 Gyr, 20 ± 5 Myr and 50 ± 10 Myr, distance moduli of 12.30 ± 0.40 , 13.80 ± 0.70 , and 12.90 ± 0.55 mag, and color excesses of 0.20 ± 0.06 , 0.90 ± 0.11 , and 0.55 ± 0.08 mag, respectively. To ensure accuracy, we applied the ASteCA (Automated Stellar Cluster Analysis) code (<https://asteca.readthedocs.io/en/latest/>), following all installation instructions (cf. [Perren et al. 2015, 2020](#)). The main results of the clusters are consistent with our visual fit except for the Dolidze 18 distance modulus, which is exceeded by about 2.10 mag of the ASteCA.

We used the absorption ratio of the photometric systems in different wavelengths to the visual absorption (A_λ/A_V), [Cardelli et al. 1989](#); [O'Donnell 1994](#); and the Padova website CMD 3.0 (http://stev.oapd.inaf.it/cgi-bin/cmd_3.0). The absorption ratios of Gaia (DR2) are $A_G/A_V=0.861$, $A_{GBP}/A_V=1.062$, and $A_{GRP}/A_V=0.651$. These ratios have been used for correction of the magnitudes for interstellar reddening and converting the color excess to $E(B-V)$, where $R_V=A_V/E(B-V)=3.1$ and $E(B-V)=0.785 E(BP-RP)$.

The parallax values of Gaia (DR2) are affected by an offset of -0.029 mas, [Lindegren et al. \(2018\)](#), which has been considered here. However, depending on the mean parallax of the clusters under study, Collinder 467, Dolidze 18, and Ruprecht 70, yield distances of 2440, 3333, 2272 pc respectively. They agree well with the CMD fitting distances of Collinder 467 and Ruprecht 70 in differences of 55 and 18 pc respectively. Although, it does not agree with the CMD fitting of Dolidze 18, where it is different by 888 pc. The members of the cluster were selected for the stars which are inside the diameter of the cluster and their parallax errors ≤ 0.15 mas, and proper motion errors ≤ 0.3 mas/yr. Correspondingly, the Cartesian galactocentric coordinates ($X_\odot, Y_\odot, Z_\odot$), and the distances from the galactic center (R_g) are estimated for the clusters under study and listed in [Table 1](#) (cf. [Tadross 2011](#)). The Y-axis connects the Sun to the Galactic center, while the X-axis is perpendicular to Y-axis. Y_\odot is positive toward the Galactic anti-center, and X_\odot is positive in the first and second Galactic quadrants ([Lynga 1982](#)).

5. Luminosity & mass functions, and dynamical state

A large number of stars of the same age and chemical structure but differing masses make up an open cluster. The luminosity and mass functions of a cluster are determined by the number of confirmed membership (LF & MF). The most difficult aspect of studying the LF and MF is removing field star pollution from the cluster's area. We can distinguish cluster members from field stars by using the cluster's true dimension, parallax, and proper motion conditions.

A high-degree polynomial equation between the absolute magnitudes and the masses of the main sequence stars can be derived from the isochrone that better fits the cluster. The distance modulus of the cluster is used to transform the apparent magnitudes of the cluster's members to absolute magnitudes. Following that, the potential masses can be determined. In the left-hand panels of [Fig. 8](#), a histogram of LF for each cluster has been

plotted. We found that the brightest, most massive stars are clustered in the cluster's center, while the fainter and less massive stars are scattered outside. The total luminosity of Collinder 467, Dolidze 18, and Ruprecht 70 are found to be -3.0 , -6.5 , and -4.7 mag, respectively. Based on the theoretical data of the applied isochrons, the members of the cluster are divided into mass intervals, which are linked to their absolute magnitude bins. The resulting MF of Collinder 467, Dolidze 18, and Ruprecht 70 are shown in the right-hand panels of **Fig. 8**. The linear fit represents the initial mass function (IMF) slope obtained from the following equation:

$$\frac{dN}{dM} \propto M^{-\alpha}$$

where dN/dM is the number of stars in the mass interval $[M: (M + dM)]$ and α is the slope of the relation, which is found to be -2.30 , -1.60 , and -2.45 , respectively. It indicates that the MF slopes of Collinder 467 and Ruprecht 70 agree well with [Salpeter \(1955\)](#) value, while the MF slope of Dolidze 18 is small relative to the Salpeter value (it indicates that most members of the cluster $< 0.5 M_{\odot}$). The total masses of the target clusters are calculated by integrating the masses of the cluster members ([Sharma et al. 2006](#)). They are found to be 320, 500, and 262 M_{\odot} , respectively. Finally, the relaxation time (T_R) of the clusters under study has been determined, where T_R is the time scale when the cluster loses all traces of its initial conditions, i.e., the time for the cluster to reach the equivalent level of energy. It is given by the formula of [Spitzer & Hart \(1971\)](#) as:

$$T_R = \frac{8.9 \times 10^5 \sqrt{N} \times R_h^{1.5}}{\sqrt{\langle m \rangle} \times \log(0.4N)}$$

where N is the number of cluster members, R_h is the radius containing half of the cluster mass (in parsecs; assuming that R_h equals half of the cluster radius), and $\langle m \rangle$ is the average total mass of the cluster. Then, T_R is found to be 28, 42, and 14 Myr for Collinder 467, Dolidze 18, and Ruprecht 70, respectively. According to the cluster age and its relaxation time, we can define the dynamical evolution parameter τ , where $\tau = \text{Age}/T_R$. The age of the cluster should be sufficiently greater than the relaxation time. This parameter indicates that Collinder 467 is dynamically relaxed, and Ruprecht 70 is recently relaxed, while Dolidze 18 is not relaxed yet.

6. Conclusions

We present here a new Gaia (DR2) analysis of the three open clusters Collinder 467, Dolidze 18, and Ruprecht 70 that have never been photometrically studied before. These clusters lie in constellations Monoceros, Auriga, and Carina, respectively. We estimated the key physical parameters of the clusters under investigation using the Gaia (DR2) database. **Table 1** summarizes the physical parameters determined in this analysis. We used the ASteCA code to ensure precision and were able to achieve more precise parameters, although the actual sizes were found to be bigger. On studying the dynamical state, we found that Collinder 467 is relaxed, and Ruprecht 70 is recently relaxed, while Dolidze 18 is not relaxed yet.

Acknowledgments

This work is a part of a project named “IMHOTEP,” program No. 42088ZK between Egypt and France. We are grateful to the Academy of Scientific Research and to the Service of scientific cooperation in both countries for allowing us to work through this project and provide the necessary support to accomplish our scientific goals. This work has used data from the European Space Agency (ESA) mission Gaia processed by (<https://www.cosmos.esa.int/web/gaia/dpac/consortium>), i.e., the Gaia Data Processing & Analysis Consortium (DPAC). Funding for the DPAC has been provided by national institutions, in particular, the institutions participating in the Gaia Multilateral Agreement.

REFERENCES

- Bossini, D. et al. 2019, *Astrophys Space Sci*, 364, 151
Bressan A. et al. 2012, *MNRAS*, 427, 127
Cantat-Gaudin, T. et al. 2020, *A&A*, 640, A1
Cantat-Gaudin, T., & Anders, F. 2020, *A&A* 633, A99
Cardelli, J., Clayton, G., & Mathis, J. 1989, *ApJ*, 345, 245
Dias, W., Alessi, B., Moitinho, A., & Lepine, J. 2002, *A&A* 389, 871
Dias, W., Monteiro H., Caetano, T, et al. 2014, *A&A*, 564-A, 79
Evans, D.W, et al. 2018, *A&A*, 616, A4
Gaia Collaboration et al. 2018, *A&A*, 616, A1
Gilmore, G., Randich, S., Asplund, M, et al. 2012, *The Messenger*, 147, 25
Jeffries, R., Thurston, M., & Hambly, N. 2001, *A&A*, 375, 863
King, I. 1966, *AJ*, 71, 64
Koposov, S., Glushkova, E., & Zolotukhin, I. 2008, *A&A*, 486, 771
Lindgren, L. et al. 2018, *A&A*, 616, A2
Lynga, G. 1982, *A&A*, 109, 213
Martinez-Medina et al. 2016, *The Astrophysical Journal Letters*, 817: L3 (6pp)
Morau, E. 2016, *EAS Publications Series*, 80, 7311
O'Donnell, J. 1994, *ApJ*, 422, 158
Perren, G., Vázquez, R., & Piatti, A. 2015, *A&A*, 576A, 6
Perren, G. et al. 2020, *A&A*, 637A, 95
Peterson, C., & King, I. 1975, *AJ*, 80, 427
Piatti, A., Claria, J. & Ahumada, A. 2010, *MNRAS*, 402, 2720
Piskunov, A. E. et al. 2006, *A&A*, 445, 545
Portegies Zwart, S., McMillan, S., & Gieles, M. 2010, *ARA&A*, 48, 431
Ruprecht, J. 1966, *Bull. Astron. Inst. Czech.*, 17, 33
Salpeter, E. 1955, *ApJ*, 121, 161
Sampetro, L., Dias, W. et al. 2017, *MNRAS*, 470, 3937
Sharma, S., Pandey A., Ogura, K. et al. 2006, *AJ*, 132, 1669
Spitzer, Lyman Jr., Hart Michael, H. 1971, *AJP*, 164, 399
Tadross, A. L. 2011, *JKAS*, 44, 1
Tadross, A. L. 2018, *RAA*, 18, 158
Tadross, A. L., & Hendy, Y. H. 2021, *JApA*, 42, 6

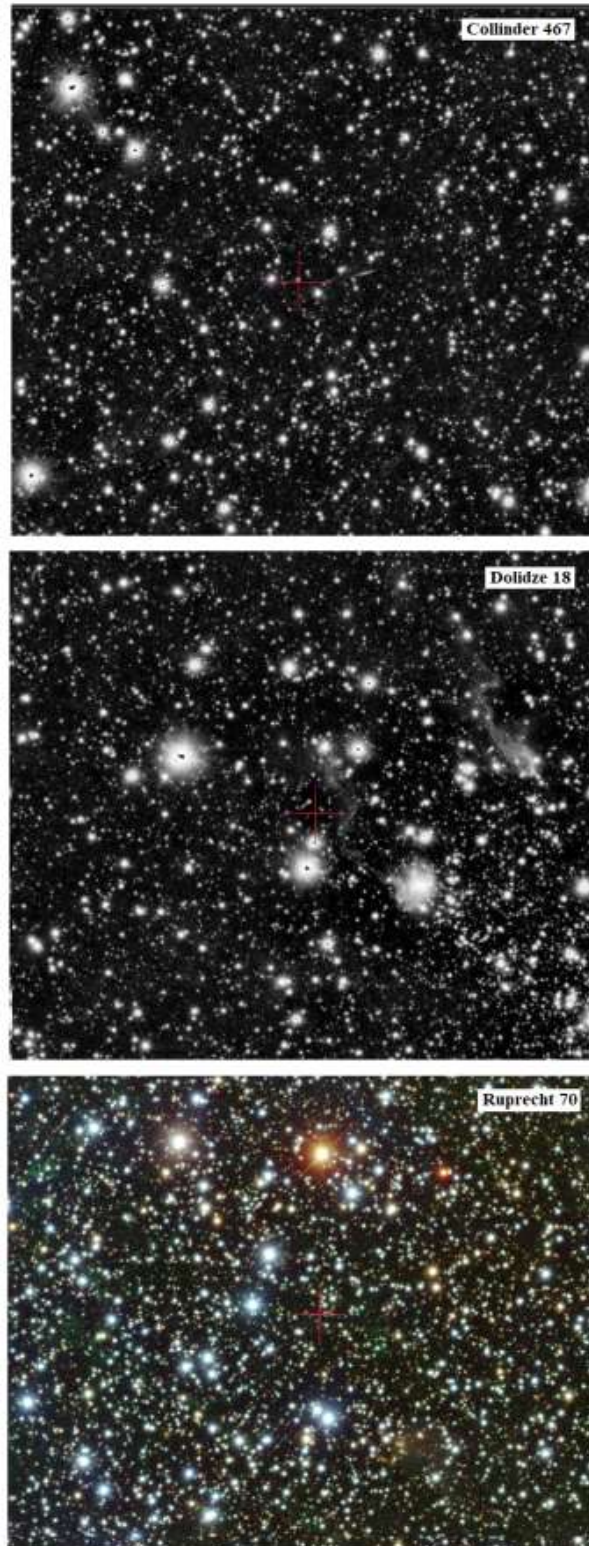


Figure 1: The images of the candidate clusters Collinder 467, Dolidze 18, and Ruprecht 70 as taken from ALADIN. These clusters lie in constellations Monoceros, Auriga, and Carina, respectively. No obvious central concentration is shown. North is up, East is to the left.

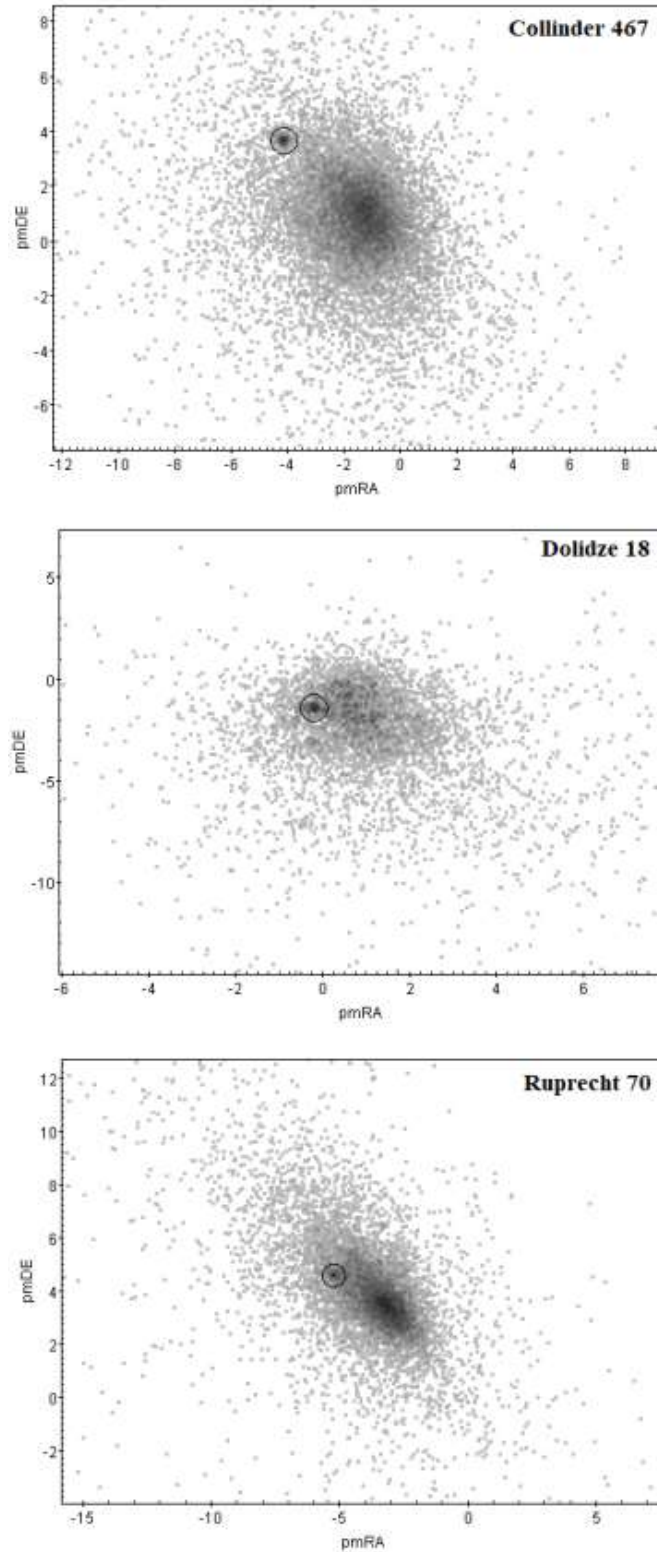


Figure 2: Vector point diagrams of the candidate clusters Collinder 467, Dolidze 18, and Ruprecht 70, from which the highest concentrated area is selected as a subset of the most probable members of each cluster. The circles refer to the most darkened areas, where the stars are selected for our study.

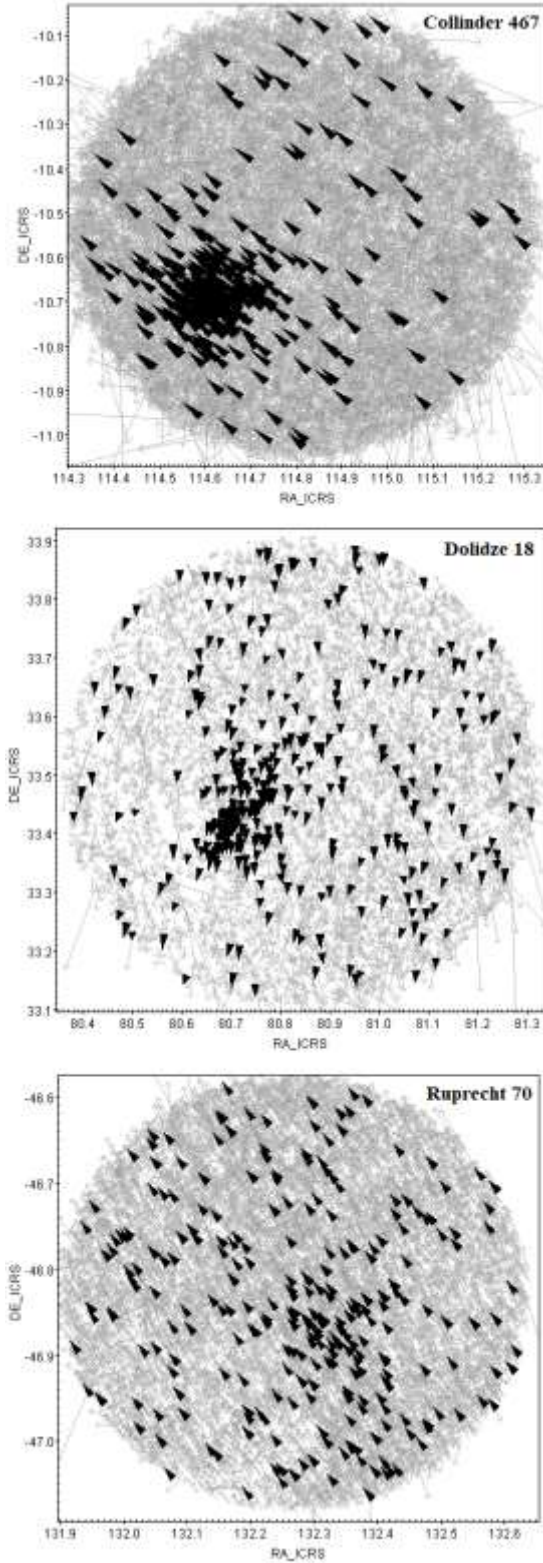


Figure 3: The comoving stars of the candidate clusters Collinder 467, Dolidze 18, and Ruprecht 70. They represent the subsets that were selected from the VPDs, i.e., the stars that move together with the same velocity in the sky.

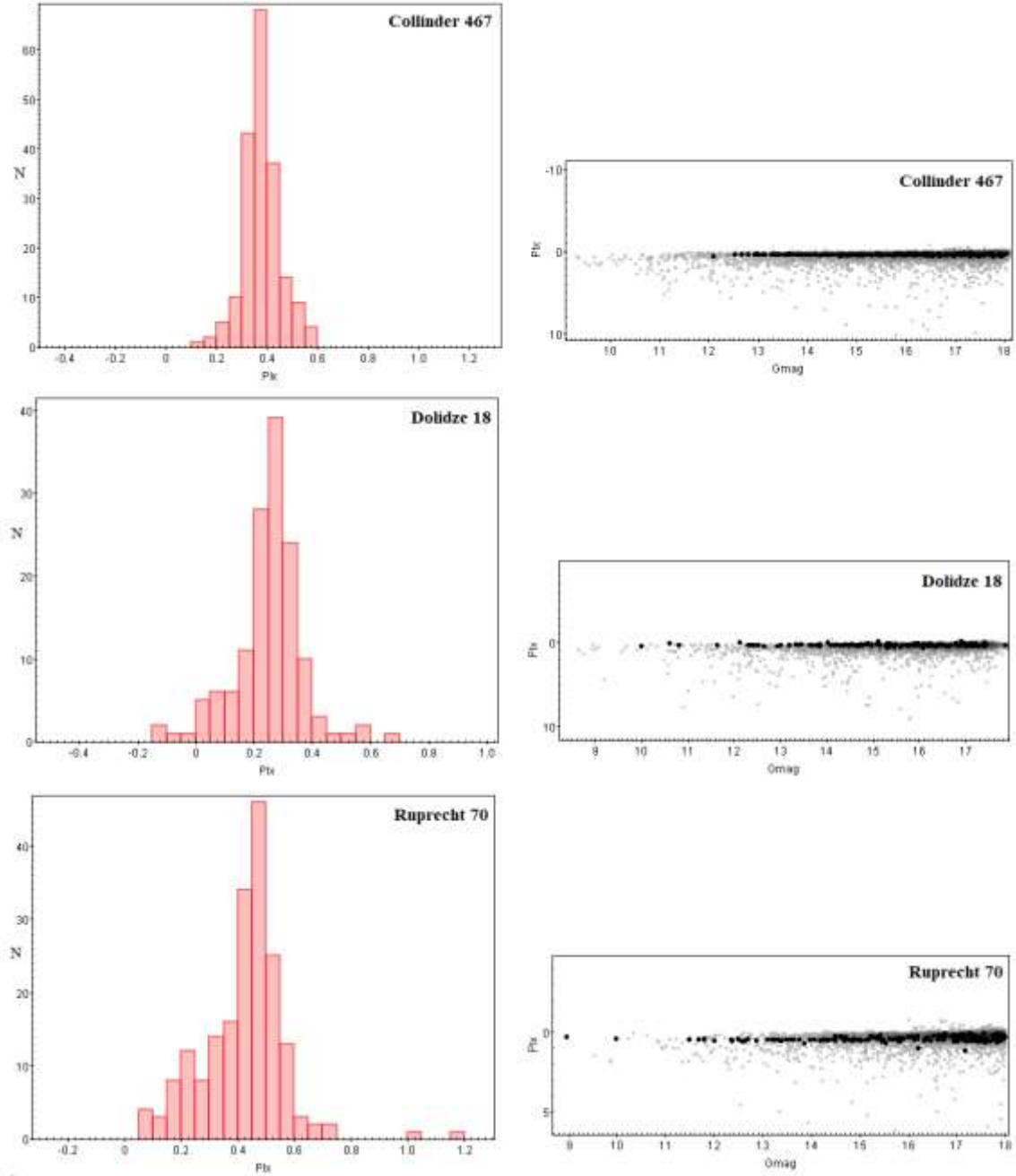


Figure 4: The left-hand panels show the parallax ranges of the candidate clusters Collinder 467, Dolidze 18, and Ruprecht 70. The right-hand panels present the relation between the magnitude and parallax of the clusters under study. It shows concentration for the members of the cluster, while the stars in the field seem to be dispersed.

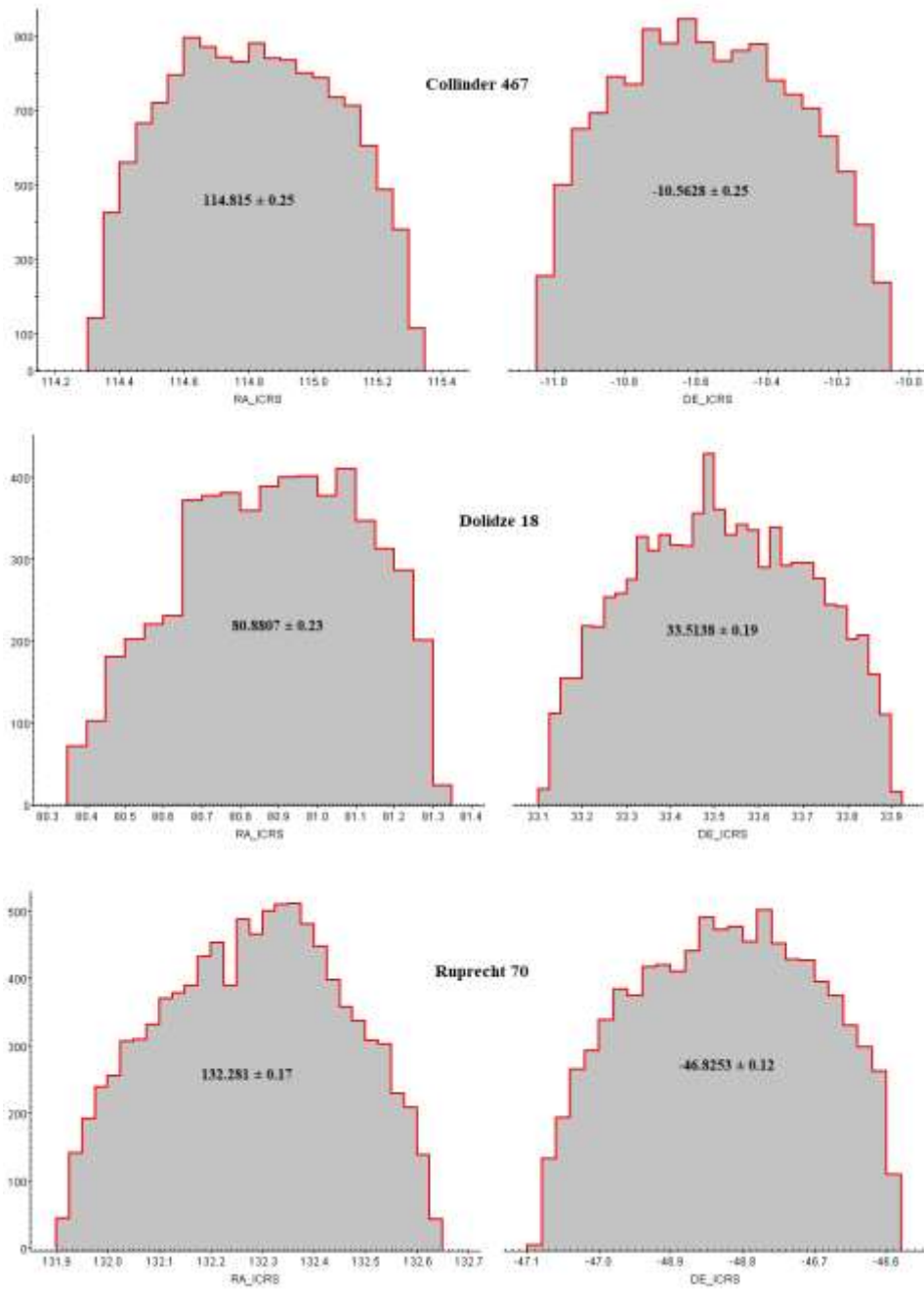


Figure 5: Centers determination of the candidate clusters Collinder 467, Dolidze 18, and Ruprecht 70. The mean values of RA and DE are estimated in degrees for each cluster, which are found to be in good agreement with Dias, see Table 1.

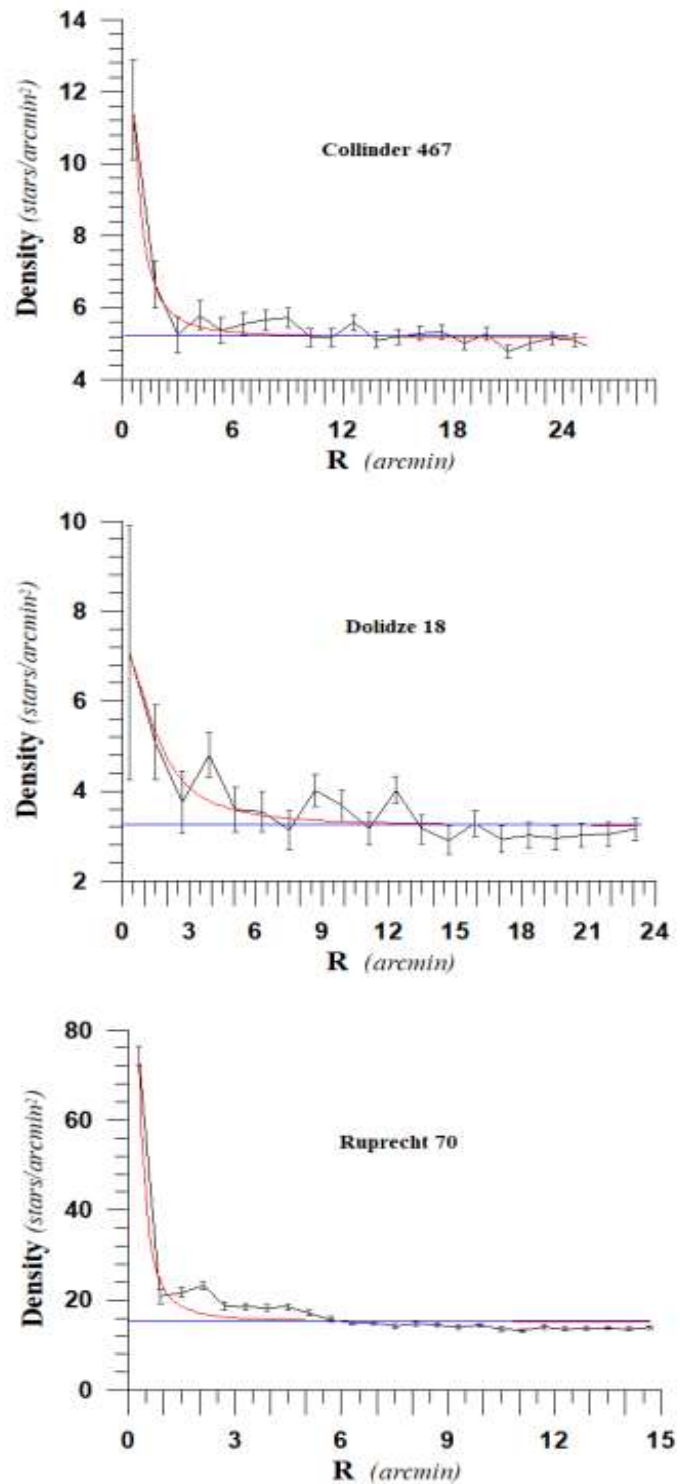


Figure 6: Radial density profiles of the candidate clusters Collinder 467, Dolidze 18, and Ruprecht 70. The error bars refer to the Poisson distribution, and the red line refers to the fitted profile of King (1966). The limited radius is found to be 10.0, 13.5, and 6.5 arcmin, respectively.

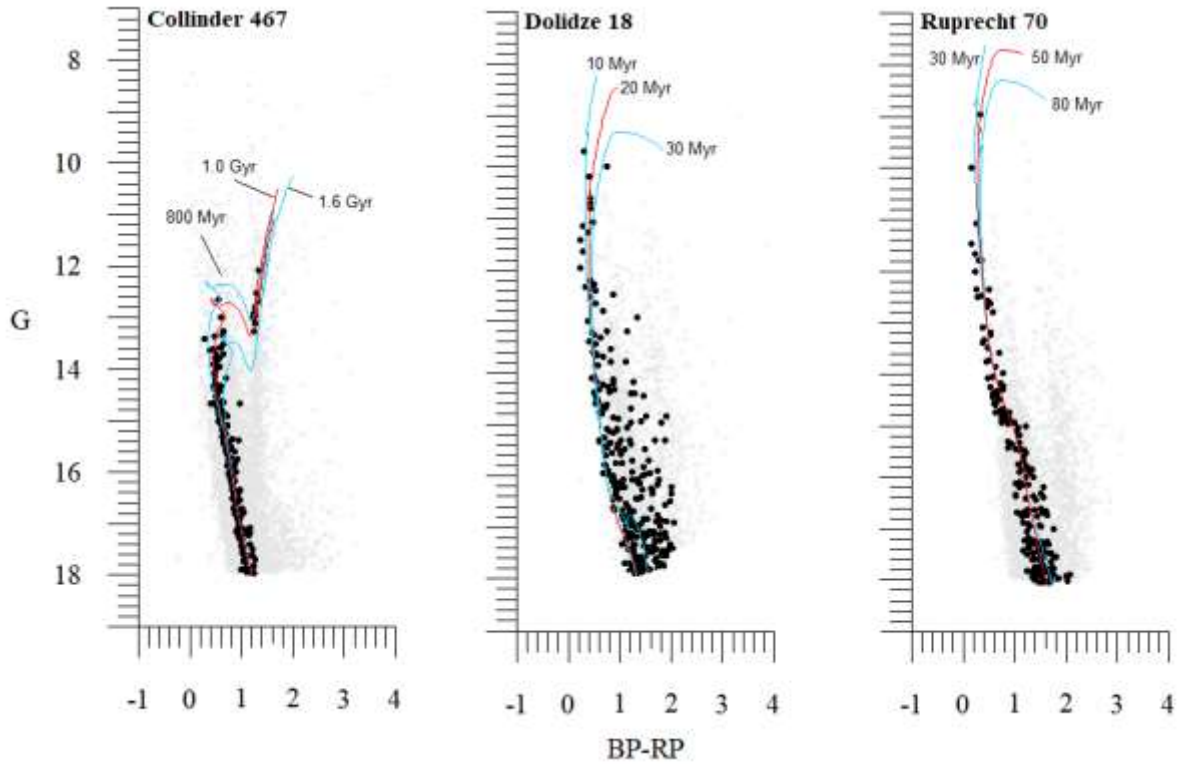


Figure 7: The theoretical isochrone of the solar metallicity $Z=0.0152$ of Padova with three different ages have been applied to each cluster. The main parameters of Collinder 467, Dolidze 18, and Ruprecht 70 are verified with ages= 1.0 ± 0.3 Gyr, 20 ± 5 Myr and 50 ± 10 Myr, distance moduli $m-M=12.30\pm 0.40$, 13.80 ± 0.70 , and 12.90 ± 0.55 mag, and color excesses $E(BP-RP)=0.20\pm 0.06$, 0.90 ± 0.11 , and 0.55 ± 0.08 mag, respectively.

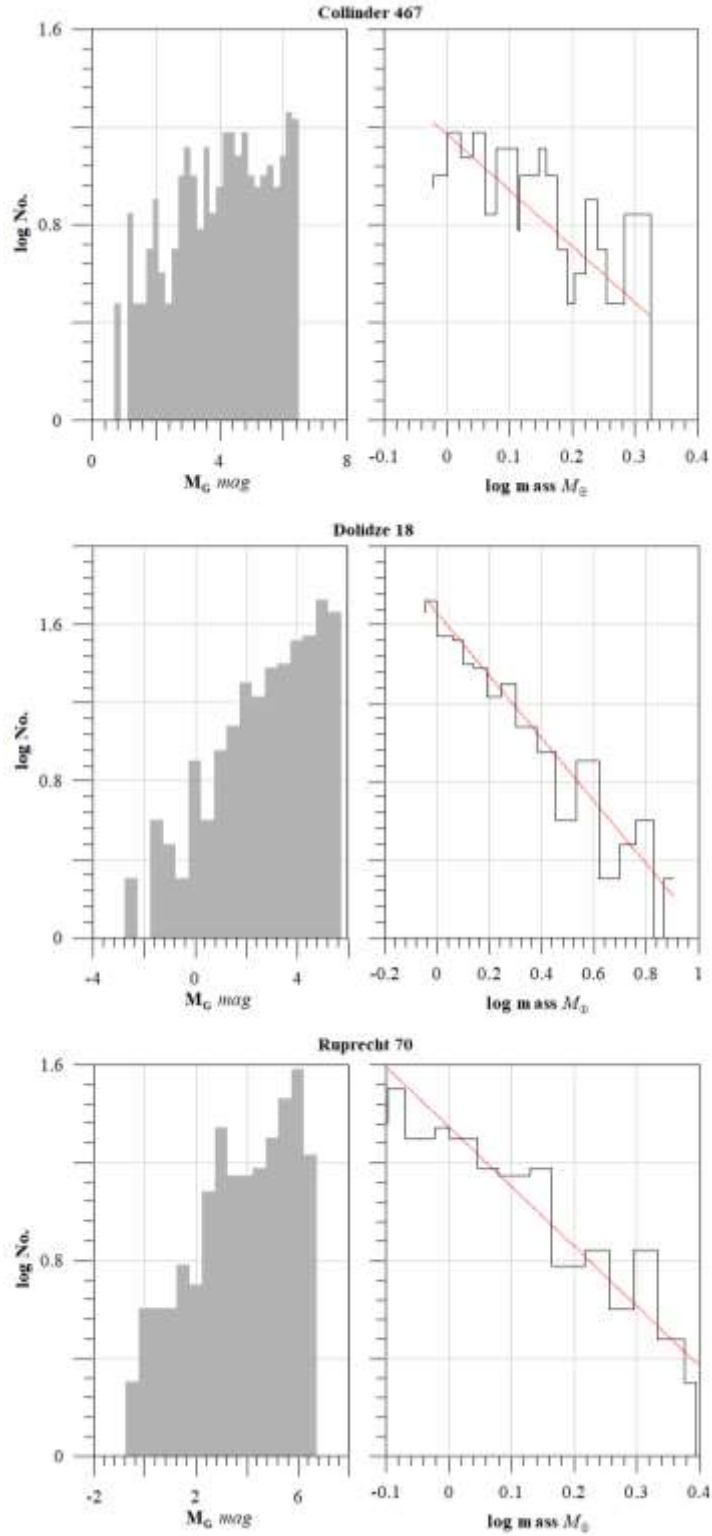


Figure 8: The left-hand panels represent the luminosity function distribution, while the right-hand panels represent the mass function distribution of the clusters under study. The red linear fit shows the slope of the relation, where $\alpha = -2.30$, -1.60 , and -2.45 , respectively.

Table 1. *The current estimate of the clusters' parameters*

Parameter	Collinder 467	Dolidze 18	Ruprecht 70
<i>a</i> (2000) deg	114.815	80.8807	132.281
δ (2000) deg	-10.5628	33.5138	-46.8253
<i>l</i> (2000) deg	227.8378	173.5937	266.3256
<i>b</i> (2000) deg	5.6039	-1.4869	-1.9140
Age	1.0±0.3 Gyr	20±5 Myr	50±10 Myr
E(BP-RP) mag	0.20±0.06	0.90±0.11	0.55±0.08
(m-M) mag	12.30±0.40	13.80±0.70	12.90±0.55
E(B-V) mag	0.16±0.06	0.70±0.11	0.43±0.08
A_G mag	0.41	1.86	1.14
A_V mag	0.50	2.20	1.30
(m-M)₀ mag	11.95±0.40	11.67±0.70	11.66±0.55
Dist. pc	2385±110	2445±150	2255±100
Plx. mas	0.41±0.09	0.30±0.12	0.44±0.14
pmRA mas/yr	-4.15±0.09	-0.21±0.06	-5.19±0.15
pmDE mas/yr	3.67±0.09	-1.41±0.13	4.63±0.12
Mem. stars	269	302	217
R_{lim} arcmin	10.0	13.5	6.5
R_c arcmin	0.67	1.6	0.2
C	1.20	0.93	1.50
R_g kpc	10.10	1077	8.78
f_{bg}	5.2	3.2	15
f_o	11.3	4.0	196
X_⊙ pc	1595	2430	144
Y_⊙ pc	-1760	274	-2248
Z_⊙ pc	233	-65	-76
R_t pc	10.00	11.60	9.30
IMF slope	-2.30	-1.60	-2.45
Total lum. mag	-3.0	-6.5	-4.7
Total mass M_⊙	320	500	262
T_R Myr	28	42	14
τ	36	0.5	3.5